Improved parameters and expanded simulation options for a model of the auditory periphery

Muhammad S. A. Zilany[1,2], Ian C. Bruce[3], Rasha A. Ibrahim[3], Laurel H. Carney[2]

[1]University of Malaya, Kuala Lumpur, Malaysia; [2]University of Rochester, Rochester, NY, USA; [3]McMaster University, Hamilton, ON, Canada

ABSTRACT

A phenomenological model of the auditory periphery in cats was previously developed by Zilany and colleagues (JASA, 2009) to examine the detailed transformation of acoustic signals into the auditory-nerve (AN) representation. In this study, a few issues arising from the responses of the previous version have been addressed. The parameters of the synapse model have been readjusted to better simulate reported discharge rates at saturation for higher characteristic frequencies (CFs). This modification also corrects the responses of higher-CF model fibers to low-frequency tones that were erroneously much higher than the responses of low-CF model fibers in the previous version. Some new simulation options are also described. First, the possibility of incorporating frozen fractional Gaussian noise in the model of the synapse has been detailed. Second, an analytical method has been implemented to compute instantaneous mean rate and variance from the model's synapse output that takes into account the effects of refractoriness. Finally, a version of the model with some parameters derived from the human auditory system is described. The revised model is more suitable to study and model psychophysical experiments with normal and impaired human listeners.

DESCRIPTION OF THE MODEL

A. Model of the Auditory-periphery

❖ The auditory-periphery model (Zilany and Bruce, 2006; Zilany et al., 2009) has most of the non-linearities seen in AN responses (e.g., nonlinear tuning, compression, sppression, level-dependent phase responses, shift in the best frequency as a function of sound level, adaptation, high level nonlinearities such as component1-component2 transition and peak-splitting).

❖ Classical models of neurotransmitter vesicle release in the inner-hair-cell (IHC)-AN synapse have the same double-exponential adaptation at both onset and offset. However, experimental data has different dynamics in the onset and offset responses. Thus, these models fail to account for responses in the stimulus offset, as well as other long-term response properties in the AN.

❖ To address the different dynamics seen in the AN onset and offset responses, the synapse model has exponential adaptation followed by power-law dynamics of adaptation (Zilany et al., 2009). This model can account for responses in the stimulus offset, long-term response properties, as well as adaptation to increments and decrements in the amplitude of an ongoing stimulus.
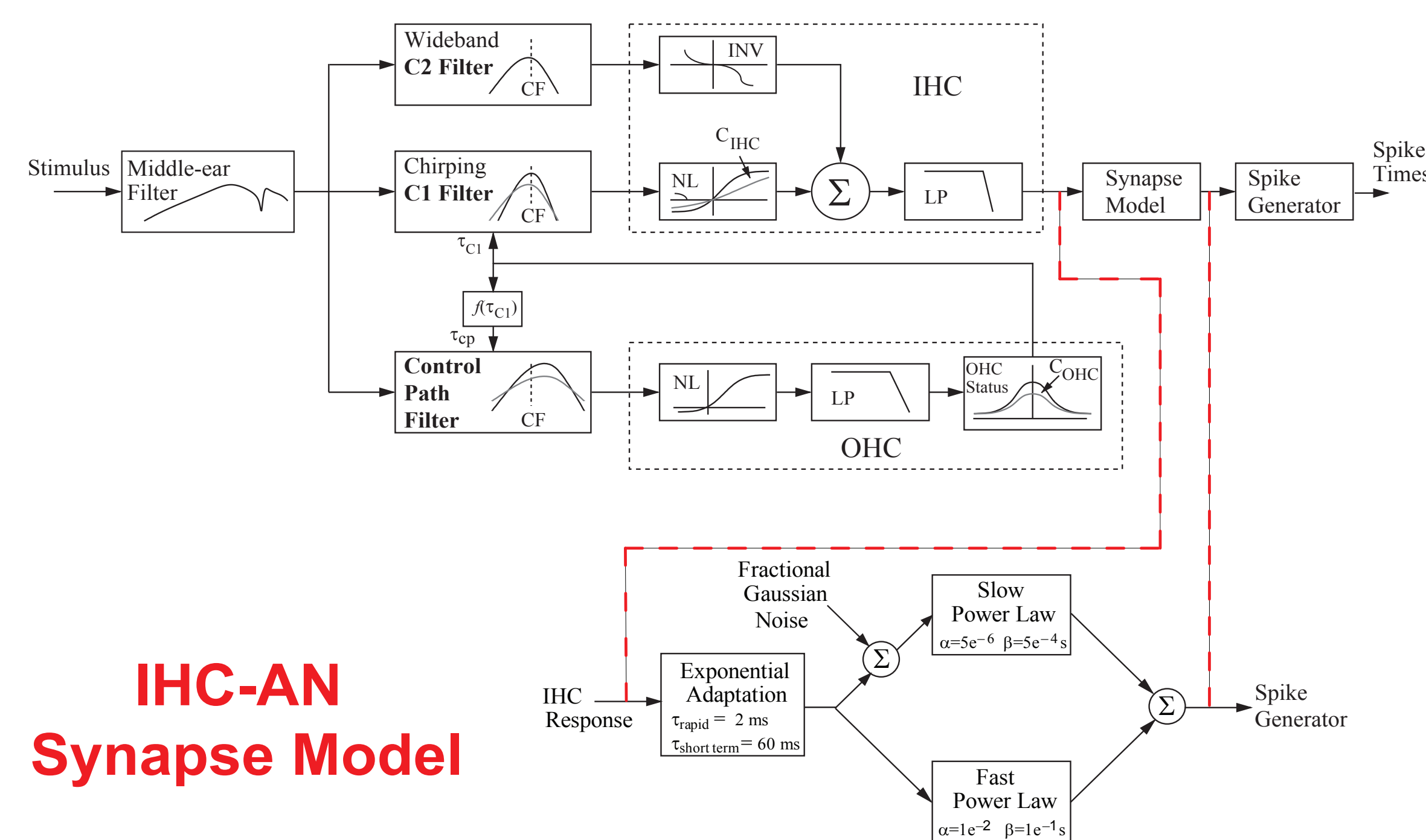

IHC-AN Synapse Model

FIG 1. Schematic diagram of the auditory-periphery model. From Zilany et al. (2009). IHC-AN synapse model: Exponential adaptation followed by parallel power law adaptation models (slow and fast). Fractional Gaussian noise (fGn) added at the input of the slow power law adaptation model results in desired distribution of spontaneous rate (SR) in the output.

B. Power-Law Synapse Model

❖ The suppressive effects, I(t), are accumulated with power-law dynamics (Drew and Abbott, 2006).

❖ The much longer tail on the power-law function produces a longer memory for past responses than does exponential adaptation.

$$r(t) = \max[0,\ S(t) - I(t)]$$
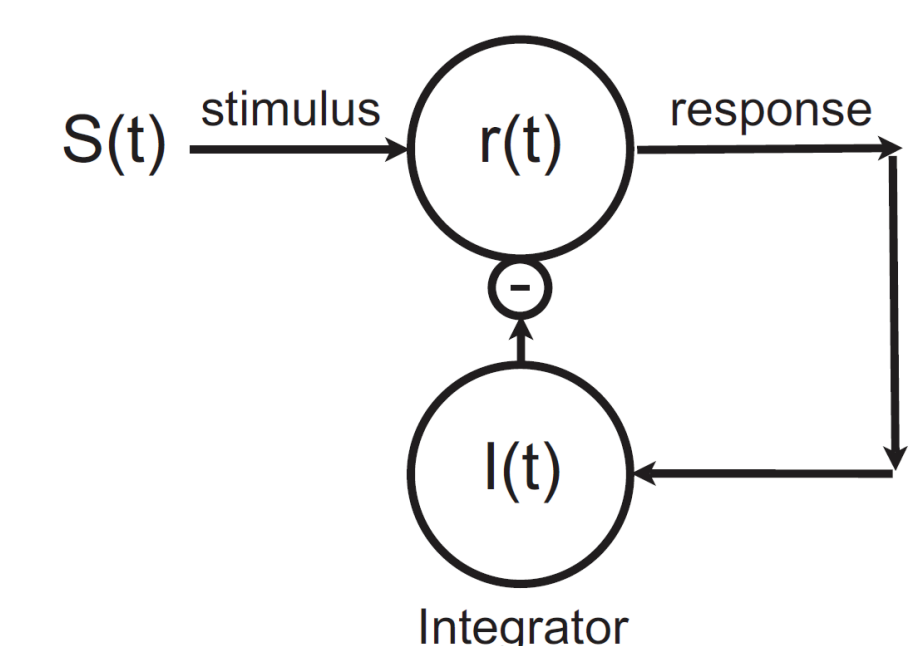
$$I(t) = \alpha \int_0^t dt' \frac{r(t')}{t - t' + \beta}$$

From Drew and Abbott, 2006

MODIFICATIONS OF THE MODEL

A. Saturation Rate as a function of CF

❖ The model saturation rates to CF tones at higher frequencies are significantly higher than the rates described by Liberman (1978).

❖ Also, the responses of higher-CF model fibers to low-frequency tones are erroneously much higher than the responses of low-CF model fibers to the same stimulus. This is evident from the response area to a 500-Hz tone signal (Fig. 2A).

❖ To solve these problems, it was necessary to readjust the parameters of the power-law model to achieve responses that agree with the cat AN data.
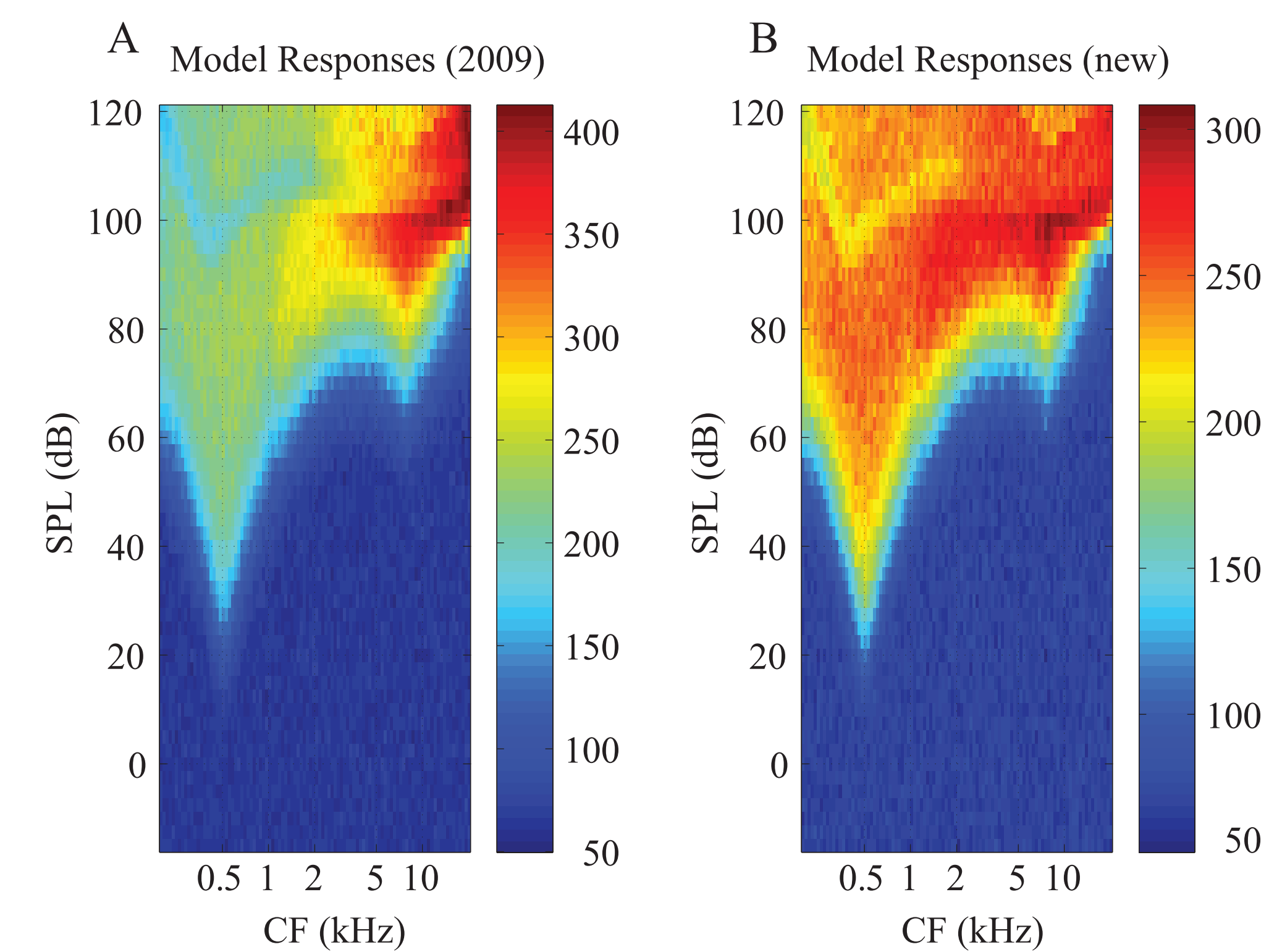

FIG 2. Responses of a population of AN model fibers to a 500-Hz tone (50-ms duration with 2.5 ms on/off ramp). Mean rate responses are shown for 100 AN fibers with CFs logarithmically spaced from 200 Hz to 20 kHz (along the x-axis) and sound levels ranging from -15 to 120 dB SPL (along the y-axis) in steps of 2.5 dB. A) Responses from the Zilany et al. (2009) model. B) Responses from the modified model presented here.

B. Implications of using frozen fractional Gaussian noise (fGn) in the synapse model

❖ Incorporation of fGn in the slow power-law path renders the model synapse output stochastic, meaning that every simulation will result in a slightly different synapse response. A fractional Gaussian noise driven Poission process can successfully model the Long-range-dependence (LRD) discharge rates of AN fibers (Teich and Lowen, 1994).

❖ As LRD significantly increases the variability of the estimates of mean rates, the histogram of the spontaneous rates (SR) as reported in Liberman (1978) can be replicated using only three true SRs (Jackson and Carney, 2005; Zilany et al., 2009).

❖ For some modeling applications, the random nature of the synapse output might be problematic. However, the advantage of having the power-law in the synapse model outweighs the inconvenience caused by the stochastic nature of the synapse output due to fGn.

❖ To avoid atypical behavior from the synapse output when using a fixed (frozen) fGn, a seed value for the MATLAB function randn has been chosen that gives fairly average behavior at the output. The effect on the response output will be equivalent to having a fixed SR instead of an SR from a distribution.

C. Estimation of instantaneous mean rate and variance from synapse output

❖ Vannucci and Teich (1978) derived a general expression for the dead-time (absolute refractory period) modified mean and variance for a counting process when the rate of input is an arbitrary function of time.
Instantaneous mean rate, $R(t) = S_{out}(t)/[1 + \tau S_{out}(t)]$,
where $R(t)$ is the mean discharge rate as a function of time, $S_{out}(t)$ is the model synapse output, and τ is the absolute refractory period (0.75 ms).

The variance of the rate can be computed as $\sigma^2(t) = S_{out}(t)/[1 + \tau S_{out}(t)]^3$

PARTIAL HUMANIZATION OF THE MODEL

❖ Middle-ear filter (Pascal et al., 1998)
❖ Basilar membrane (BM) tuning (Shera et al., 2010)
❖ Frequency offset of control path (Greenwood, 1990)
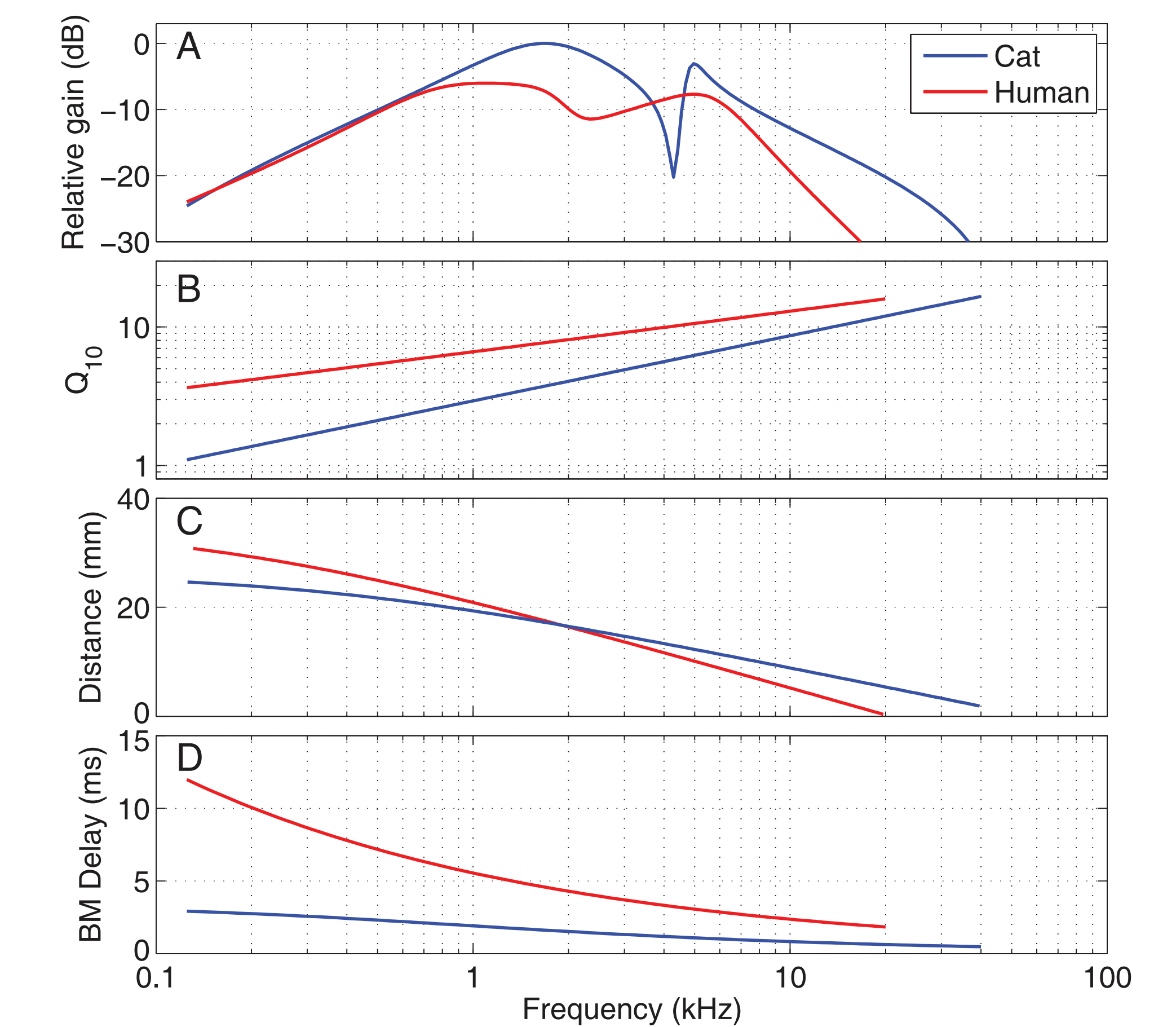❖ BM delay (Harte et al., 2009)

FIG 3. Comparison of human and cat versions of some model sections. A) Middle-ear filter frequency responses. B) Q_{10} versus CF functions. C) BM place (distance from stapes) versus CF functions. D) BM delay versus CF functions.

DISCUSSION

❖ A revised phenomenological model of the auditory periphery is presented here.
❖ The changes made to the previous version (Zilany et al., 2009) corrected the model saturation rates as a function of CF without adversely affecting other response properties. The forward-masking properties were affected to a small degree, as could be expected after modifying synaptic adaptation.
❖ To avoid the stochastic nature of the synapse output, the model included an option to simulate responses with a fixed fGn.
❖ The revised model also included a set of parameters that describes the middle-ear transfer function and peripheral tuning in human.
❖ The model is now a better candidate to examine realistic neural-encoding hypotheses, especially those involving higher CFs.

References

[1] Zilany, M. S. A., Bruce, I. C., Nelson, P. C., and Carney, L. H. (2009) "A phenomeno-logical model of the synapse between the inner hair cell and auditory nerve: long-term adaptation with power-law dynamics," J. Acoust. Soc. Am., 126, 2390–2412.

[2] Zilany, M. S. A. and Bruce, I. C. (2006). "Modeling auditory-nerve responses for high sound pressure levels in the normal and impaired auditory periphery," J. Acoust. Soc. Am., 120(3), 1446–1466.

[3] Drew, P. J. and Abbott L. F. (2006). "Models and properties of power-law adaptation in neural system," J. physiol, 96, 826–833.

[4] Teich, M. C., and Lowen, S. B. (1994). "Fractal patterns in auditory nerve spike trains," IEEE Eng. Med. Biol. Mag. 13, 197–202.

[5] Liberman, M. C. (1978). "Auditory-nerve response from cats raised in a low-noise chamber," J. Acoust. Soc. Am. 63(2), 442–455.

[6] Jackson, B. S., and Carney, L. H. (2005). "The spontaneous-rate histogram of the auditory nerve can be explained by only two or three spontaneous rates and long-range dependence," J. Assoc. Res. Otolaryngol. 6, 148–159.

[7] Vannucci, G., and Teich, M. C. (1978). "Effects of rate variation on the counting statistics of dead-time-modified Poisson processes," Optics Communications 25(2), 267–272.

[8] Pascal, J., Bourgeade, A., Lagier, M., and Legros, C. (1998). "Linear and nonlinear model of the human middle ear," J. Acoust. Soc. Am. 104, 1509–1516.

[9] Shera, C. A., Guinan Jr., J. J., and Oxenham, A. J. (2010). "Otoacoustic estimation of cochlear tuning: validation in the chinchilla," J. Assoc. Res. Otolaryngol. 11, 343–365.

[10] Greenwood, D. D. (1990). "A cochlear frequency-position function for several species – 29 years later," J. Acoust. Am. 87, 2592–2605.

[11] Harte, J. M., Pigasse, G., and Dau, T. (2009). "Comparison of cochlear delay estimates using otoacoustic emissions and auditory brainstem responses," J. Acoust. Soc. Am. 126, 1291–1301.